JCTC Journal of Chemical Theory and Computation

Article

pubs.acs.org/JCTC

Is the Tamm-Dancoff Approximation Reliable for the Calculation of Absorption and Fluorescence Band Shapes?

Agisilaos Chantzis,[†] Adèle D. Laurent,[†] Carlo Adamo,[§,‡] and Denis Jacquemin*[,†,‡]

[†]Laboratoire CEISAM-UMR CNR 6230, Université de Nantes, 2 Rue de la Houssinière, BP 92208, 44322 Nantes Cedex 3, France

[‡]Institut Universitaire de France, 103 bd Saint-Michel, F-75005 Paris Cedex 05, France

[§]Laboratoire LECIME, CNRS UMR-7575, Chimie-ParisTech, 11 rue Pierre et Marie Curie, F-75231 Paris Cedex 05, France

Supporting Information

ABSTRACT: The reliability of the Tamm−Dancoff approximation (TDA) for predicting vibrationally resolved absorption and emission spectra of several prototypical conjugated molecules has been addressed by performing a series of extensive theoretical calculations. To this end, we have systematically compared the TDA results with the full Time-Dependent Density Functional Theory (TDDFT), the Random Phase Approximation (RPA), as well as the Configuration Interaction Singles (CIS) methods that are routinely employed for the prediction of optical spectra of large molecules. Comparisons have been made with experimental results for both the band shapes and 0−0 energies. They revealed that TDA is generally able to reproduce the experimental band shapes along with the positions of the absorption and emission peaks. With respect to TDDFT, TDA leads to an underestimation of the relative intensities for most cases but does not alter any other feature of the spectra. For the case of 0−0 energies, it leads to a better agreement between theory and experiment compared to TDDFT for the majority of the molecules studied, at least when combined with the popular B3LYP functional.

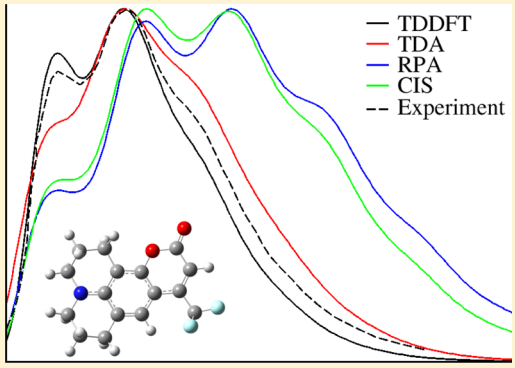

1. INTRODUCTION

It is without dispute that the advent of Time-Dependent Density Functional Theory (TDDFT) has revolutionized the domain of electronic spectroscopy of large molecules (up to ca. 500 atoms). In fact, the time-dependent extension of traditional DFT allows, with reasonable accuracy, studying the excited-state energies, geometries, and other properties of large molecules with a moderate computational cost compared to electron-correlated wave function methods. These advantages partly explain the increasing number of reviews and monographs[1−15] steadily appearing over the years. For the vast majority of spectroscopic studies, Casida's linear response approximation[16] to TDDFT in the frequency domain is used, although real-time propagation schemes have appeared and have been recently applied to molecular systems.[17−21]

Although the formal foundations of TDDFT have been proposed by Runge and Gross almost 30 years ago,[22] still, up to now, approximations have to be introduced to render it applicable to real-life problems. This is mainly due to the inability to obtain the exact exchange-correlation functional (XCF) and the frequency independence of the corresponding kernel (the so-called adiabatic approximation). These approximations have been shown to be responsible for some characteristic failures of TDDFT, for example in the treatment of long-range charge-transfer (CT) excited states,[23] double excitations,[24,25] conical intersections, and avoided crossings[26−29] or for cases exhibiting the triplet instability problem.[30−33] In some of these cases, for example, the singlet−triplet transitions of "unstable" systems, an approximation to TDDFT, the so-called Tamm-Dancoff approximation[31] (TDA) provides more accurate results.[34−37] Besides these technical advantages of TDA, it also offers very significant computational effort savings, a characteristic of great importance when very large molecules are considered. Indeed, in relation to excited state properties and geometry optimizations, full TDDFT simulations can be notoriously time-consuming and TDA provides an attractive alternative.

As mentioned previously, TDDFT, as its ground-state counterpart, does not offer an unique and systematic way to improve the quality of the obtained results, and extensive benchmark studies have been performed in order to analyze the pros and cons of different XCFs. In conjunction to the simulation of optical properties of molecules, an increasing number of systematic and high-quality benchmarks have indeed appeared, a comprehensive account of which can be found in recent articles and reviews.[38−42]

As far as optical spectra are concerned, the majority of studies involving the simulation of absorption and emission electronic spectra adopt the vertical approximation, which is based on the assumption that the nuclear degrees of freedom are frozen during an electronic transition and only the electronic degrees of freedom are of relevance. The approximation is particularly popular, especially for large

Received: July 9, 2013
Published: August 21, 2013

   dx.doi.org/10.1021/ct400597f | J. Chem. Theory Comput. 2013, 9, 4517−4525

molecules due to its simplicity, since hundreds of states can be computed within just one single-point TD calculation and no geometry optimization for the excited state of interest is required. Despite this popularity, the vertical excitation energies are not the most relevant quantities to be compared with the experimental wavelengths of absorption and emission. Recent studies[43−45] have shown that adiabatic excitation energies along with band shapes are more appropriate for mimicking experiment. Their determination, though, is hampered by the need to compute the Hessian of the excited state, an endeavor that can be extremely demanding. Only recently, the analytical calculation of excited state Hessians has been implemented and tested on very small systems (up to ca. 10 atoms),[46−48] and most TD Hessian calculations are still done numerically.

Although the calculation of adiabatic energies only requires the location of the minimum of the excited state potential energy surface (PES), the prediction of the band shapes requires, according to the Franck−Condon (FC) approximation,[49,50] the computation of the overlap integrals between harmonic vibrational wave functions. For strongly electric dipole allowed transitions the aforementioned FC approximation is adequate. For the case of weakly allowed or dipole forbidden ones, one has to consider the dependence of the electronic transition dipole moment on the normal coordinates, introducing thus the Herzberg−Teller (HT) terms.[51] The inclusion of the HT corrections requires the calculation of the first derivative of the electric transition dipole moment with respect to the normal coordinates and thus is more demanding compared to the FC treatment. In any case, one of the major problems in the computation of vibronic spectra is the proper convergence of the vibronic spectra with respect to the number of vibrational states. In one of the most popular formalisms for their computation,[52−54] a prescreening method is applied utilizing the concept of classes to select the transitions between the vibrational states that significantly contribute to the total intensity of the spectrum while convergence is monitored by applying analytic sum-rules. Therefore, a rigorous way to check the reliability of the obtained results can be straightforwardly applied. Approximations to the basic formalism can lead to different models and comprehensive investigations, along with the necessary comparisons that have been published recently.[55,56]

Despite the great number of benchmarks involving TDDFT, TDA is not extensively employed, although there are some studies investigating the predictive capability of the latter for the simulation of optical spectra.[31,34,36,57,58] In the aforementioned works, the focus was primarily on vertical transition energies of compounds belonging to organic, inorganic, and organometallic chemistry and ranging in size from diatomics to extended structures. Although comparisons with experiment and other electronic structure methods have been performed, no calculations have been attempted in order to question the predictive capability of TDA in simulating vibrationally resolved electronic spectra. Therefore, to the best of our knowledge, the present contribution is the first to address the ability of TDA to reproduce the experimental vibrationally resolved electronic spectra corresponding to transitions between the ground and the first excited state of a significant series of medium-sized conjugated molecules (see Scheme 1). To this end, we have performed systematic comparisons with TDDFT and also with both Configuration Interaction Singles[59,60] (CIS) and the Random phase Approximation[61,62] (RPA) methods. It is important to note that the methods mentioned above are closely related in the sense that TDA and CIS can be formally derived from TDDFT and RPA, respectively, by discarding the deexcitation matrix from the working equations.[7] Therefore, comparisons between these four methods can provide important insights on the adequacy of the underlying approximations that are relevant to the simulation of optical spectra.

Scheme 1. Representation of the Investigated Molecules

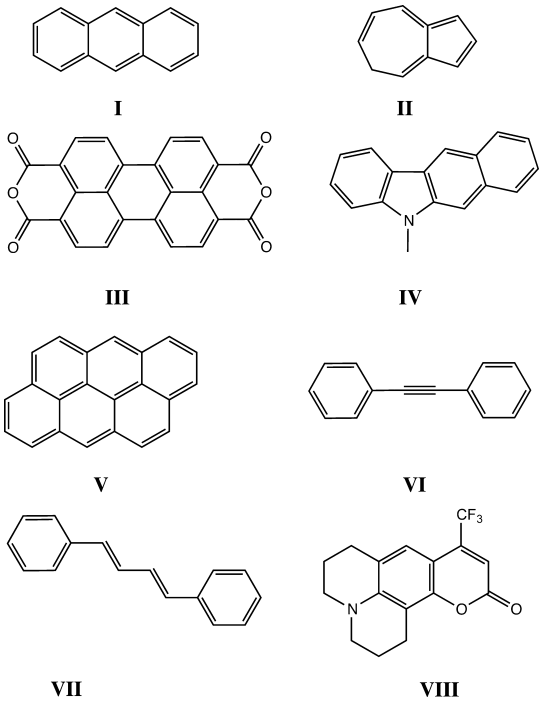

2. COMPUTATIONAL DETAILS

The basic strategy pertaining to our computational methodology, along with the definition of all the relevant quantities considered herein, has been presented elsewhere[40] and therefore will not be repeated in full detail. In fact, the molecules considered here are a subset of the ones investigated in ref 40, and therefore, we have relied on previous findings in the present study. Solvation effects on the band shapes were not considered, since they were not of immediate interest in the present case and have been treated in ref 40.

The study was performed by employing the CIS, RPA, TDDFT, and TDA methods as implemented in the Q-Chem suite of programs.[63] For the TDDFT and TDA calculations, we have chosen to use the popular B3LYP[64,65] functional for all molecules considered, since they are rather compact and long-range corrections are expected to be small. In addition, it was shown that in the TDDFT approximation, it yields vibronic spectra with the smallest (average) deviations with respect to experiment.[40] Nonetheless, we have also considered the three popular long-range corrected functionals ωB97,[66] ωB97X-D,[67] and CAM-B3LYP[68] for molecule VI to confirm the validity of our findings, beyond a single functional. For the TDDFT benchmark calculations, as well as for the calculations performed with environmental modeling (see below), Gaussian09[69] has been used. For the numerical integral computations, the standard Euler−Maclauren−Lebedev (99, 590) grid has been used, which consists of 99 radial points and 590 angular points per radial point. For some of the molecules,

this grid has proven to be computationally expensive and the standard (75, 302) has been applied, since it has been found to be adequate for determining band shapes.[40] Concerning the choice of the basis set, we have relied on the popular split-valence, double-ζ quality 6-31+G(d), which has been systematically employed for all methods reported here. For both the ground state (GS) and excited state (ES) geometry optimizations, Baker's eigenvector-following (EF) algorithm[70] was used as implemented in Q-Chem 4.0.1 and the thresholds for convergence were set to (the default) 3.0×10^{-4} au and 1.2×10^{-3} au for the maximum gradient component and the maximum atomic displacement, respectively. In order to validate that the obtained geometries correspond to real minima of the PES for both the GS and ES as well as to compute vibronic couplings, a full (harmonic) vibrational frequency analysis has been performed by computing the Hessian analytically for the B3LYP functional. For all other calculations, the ES Hessian was computed numerically.

For the calculation of the vibrationally resolved spectra, the FCclasses program[71] was used. In this work, the Franck–Condon approximation was adopted, for which it is assumed that the electronic transition dipole moment is a constant quantity. The transitions considered were strong enough so that higher-order corrections, such as Herzberg–Teller terms, were not considered. The resulting stick spectra were convoluted with Gaussian functions having the appropriate half width at half-maximum (HWHM) for a meaningful comparison with experiment (typically values of 10^{-2} eV order of magnitude). The number of overtones for C_1 class transitions was set to 25, while for C_2 class transitions the corresponding number was set to 20. As already mentioned in the Introduction, full convergence of the vibronic spectrum has to be achieved if reliable results are to be obtained. In FCclasses the accuracy of the calculations is governed by the number of integrals that are computed. Of course, this number may differ from one molecule to the other, and tests were performed so as to ensure that the spectra were fully converged (see the Supporting Information, SI). Specifically, we have checked that the number of computed integrals is sufficient to achieve a FC_{00} overlap (the overlap integral between the ground vibrational states of the initial and final electronic states) that exceeds 10^{-4}. Additionally, we have also checked that the determinant of the transformation matrix (which expresses the projection of the normal modes of one electronic state on those of the other) is, in all cases considered, close to 1 while the FC factor remains always above 0.9.

Since the relative performance of the methods employed with respect to the 0–0 energies was of no interest when comparing the band line shapes, we have systematically set the maxima of the first absorption and emission bands at the origin, and in order to facilitate comparisons, we have transformed the absolute intensities to relative ones. Additionally, we have mirror-transformed the emission spectra for easier comparisons, with the corresponding absorption ones. It has to be noted finally that the experimental fluorescence spectra have been transformed from the wavelength to the wavenumber scale by applying an intensity correction[72] proportional to the square of the frequency (ω^2). A more detailed exposition on how appropriate comparisons between theory and experiment should be conducted can be found in ref 73. The experimental data have been obtained from a series of publications.

3. RESULTS

3.1. 0–0 Energies. In this section, we summarize the results regarding the calculation of 0–0 energies. A problem one has to face is the fact that all theoretical calculations have been performed in the gas phase while almost all experimental estimates of 0–0 energies (except for **I** and **VIII**) reported herein where taken in solution. One possible solution to this problem is to correct the theoretical values for the effects of the solvent by computing the solvatochromic shifts. We have estimated the latter by means of the following equation at the TDDFT/B3LYP/6-31+G(d) level of theory

$$\Delta E^{\mathrm{solv}}(\mathrm{SS,\ neq}) = E^{\mathrm{AFCP\text{-}solv}}(\mathrm{SS,\ neq}) - E^{0-0,\mathrm{gas}}$$

where ΔE^{solv}(SS,neq) is the solvatochromic shift correction to the 0–0 energy, $E^{\mathrm{AFCP\text{-}solv}}$(SS,neq) is the theoretical analogue of the absorption/fluorescence crossing point, and $E^{0-0,\mathrm{gas}}$ is the gas phase 0–0 energy. The indication (SS,neq) indicates that the corresponding quantities were calculated using the Polarizable Continuum Model (PCM) solvation approach[74] within the state-specific (SS) formalism[75] in the nonequilibrium limit. Solvents used are given in Table 1. The solvatochromic corrections for molecule **II**–**VII** are summarized in Table 2. These corrections were subsequently applied to correct the gas phase theoretical 0–0 energies for all methods employed. In order to test the validity of our approach, we have calculated the exact solvatochromic shift for the case of **VI**, which is considered in a polar medium. For this molecule, the difference between the RPA and TDDFT corrections was found to be as small as 0.008 eV. Therefore, it is a valid first-order approach in estimating the AFCP in solution from gas phase data. Note that, for **VIII**, we also calculated a solvatochromic shift (methylpentane-gas) and found a significantly different value for RPA and TDDFT, and this is related to the CT nature of the transition. For coumarins, the difficulty to obtain a meaningful solvatochromic shift with uncorrelated method is discussed elsewhere.[83] Of course, we considered the gas phase

Table 1. List of Solvents Used in Experiment Along with the Corresponding References

molecule	solvent	ref
I	gas	76, 77
II	cyclohexane	78
III	dimethylsulfoxide	79
IV	ethanol	80
V	benzene	80
VI	ethanol	81
VII	hexane	81
VIII	gas	82

Table 2. Calculated Solvatochromic Shifts at the TDDFT/B3LYP/6-31+G(d) Level of Theory (in eV)

molecule	$E^{\mathrm{AFCP\text{-}solv}}$ (SS,neq)	$E^{0-0,\mathrm{gas}}$	ΔE^{solv} (SS,neq)
II	1.958	1.964	−0.006
III	2.173	2.214	−0.041
IV	2.840	3.057	−0.217
V	2.602	2.596	0.006
VI	3.800	3.748	0.051
VII	3.188	3.177	0.011

dx.doi.org/10.1021/ct400597f | J. Chem. Theory Comput. 2013, 9, 4517–4525

values for **VIII**, so that this problem does not influence our data here.

The 0−0 energies, or more precisely the estimation of the AFCP, for all theoretical methods along with the experimental estimates are gathered in Table 3. The experimental values were calculated as absorption-fluorescence crossing points (AFCP). For the cases where experimental fluorescence spectra were not available, the maximum of the first absorption band was taken as reference. For **I**, it was taken from ref 77. Starting from a comparison between the different theoretical methods (see Table 3), it becomes evident that very clear-cut trends emerge. Ignoring deexcitations in TDDFT leads to an increase of the calculated 0−0 energies for all molecules considered, as can be readily seen from the TDA results. Exactly the same trend is observed by going from the RPA to the CIS. Interestingly enough, starting from TDDFT and ending to CIS from left to right in Table 3 induces a sequential increase of the 0−0 values, for all molecules considered. The largest difference between TDDFT and TDA values occurs for molecule **III** (13% of the TDDFT value, ca. 0.3 eV) while for the RPA and CIS ones, the largest deviation is observed for molecule **V** (12% of the RPA value, ca. 0.3 eV). It can be concluded that the omission of deexcitations leads to a small but by no means negligible increase of the values for the 0−0 energies.

Table 3. Theoretical 0-0 Energies (Corrected for the Solvent Shift) Calculated With the 6-31+G(d) Atomic Basis Set Along with the Experimental Values (in eV)

molecule	TDDFT	TDA	RPA	CIS	exptl.
I	2.917	3.193	3.501	3.890	3.44
II	1.958	2.035	2.397	2.642	1.78
III	2.173	2.457	2.840	3.154	2.38
IV	2.840	2.970			3.10
V	2.602	2.883	3.180	3.566	2.85
VI	3.800	4.010	4.350	4.648	4.17
VII	3.188	3.520			3.55
VIII	2.898	3.019	4.115	4.397	3.16

From the comparison between theory and experiment, one can see that, except for molecule **II**, the TDA estimates are closer to experiment than TDDFT ones. Such a trend does not exist for the case of the RPA/CIS pair for which the omission of deexcitations overestimates even more the already overestimated RPA values. Although for some cases, for example for **I** RPA is in very good agreement with experiment, this can be considered fortuitous; for the case of **II**, RPA overestimates the experimental value by more than 0.6 eV. For TDDFT the errors, in absolute terms, with respect to the experiment are equal or below 15% while for TDA, the errors are, for most cases, smaller. It should be reminded though, that this outcome is related to the use of the B3LYP functional that leads to too small transition energies in the TDDFT framework (see ref 45). Using other exchange-correlation functionals might well lead to larger theory-experiment deviations with TDA than TDDFT. The performance of RPA and CIS is quite erratic and unreliable since in some cases the differences can reach up to 35% and 48% of the experimental value, respectively.

3.2. Vibronic Band Shapes. In this section, we report the vibrationally resolved electronic spectra for some of the molecules whose spectra proved to be the most representative of the whole set. The remaining are presented in the SI. It has to be noted that the spectra are fully converged except for the RPA and CIS ones for **VIII** for which the FC factors were found to be less than 0.9. Nonetheless, we have also included them in the present work for the sake of completeness.

Molecule **I**, anthracene (see Figure 1), is a common representative of polycyclic aromatic hydrocarbons and possesses a well-structured absorption spectrum. Therefore, it is an ideal candidate for theory/experiment comparisons. The experimental spectrum is composed of five principal absorption peaks that are very well resolved. It is evident from Figure 1 that all theoretical methods are able to accurately predict the positions of all five maxima, with variations of the relative intensities, though for the last one TDDFT and TDA are closer to the experimental shape than the other two noncorrelated methods. Both TDDFT and TDA correctly predict that the first band is the most intense (red and black curves overlap almost perfectly), while the Hartree−Fock variants, RPA and CIS, show that the third one is the most intense, a clear qualitative mismatch. Moreover, except for the case of the first two peaks, RPA and CIS give intensities that are larger compared to both TDDFT and TDA ones. Turning to a comparison on the one hand between TDDFT and TDA, and on the other hand between RPA and CIS, it is evident that the more approximate variants do not alter the shape of the spectrum but change only the relative intensities. Invoking the TDA approximation leads to a lowering of the intensities for the last four bands. For the case of CIS the behavior is more complicated and one can witness that for the first band's maximum the relative intensity is higher than the corresponding RPA one, the reverse being true for the two last ones. For emission, the experiment predicts that the spectrum, as in the case of absorption, is composed of five peaks. The first one is the most intense, a feature that is

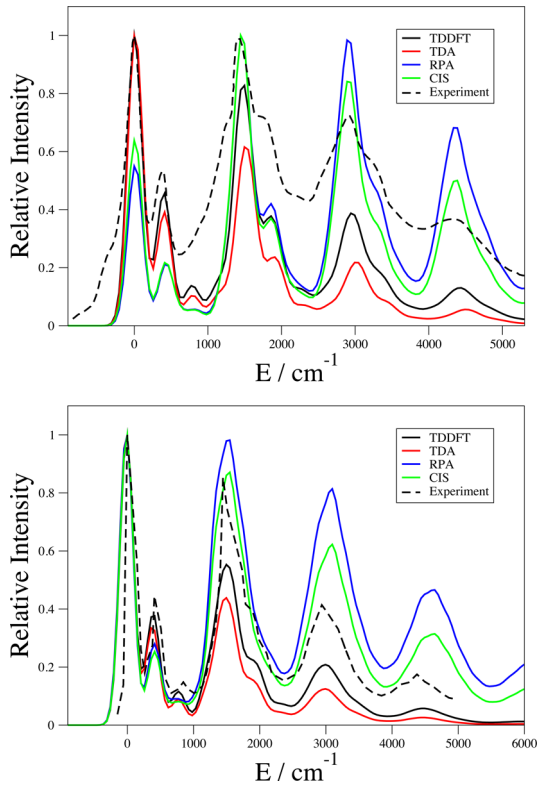

Figure 1. Comparison of the experimental and computed absorption (top) and emission (bottom) spectrum of **I** using the 6-31+G(d) basis set.

dx.doi.org/10.1021/ct400597f | J. Chem. Theory Comput. 2013, 9, 4517−4525

readily reproduced by all methods. For the second, both TDDFT and RPA underestimate slightly the intensity while RPA and CIS underestimate it even more. Ignoring deexcitations for TDDFT and RPA leads to a lowering of the relative intensities for this second peak, while leaving its position practically unaltered. It is interesting to note that as can be seen for the case of the third peak, although RPA and CIS better match the experimental results, they are unable to reproduce the close lying shoulder-like peak, a subtle feature reproduced by both TDDFT and TDA. For the region of the spectrum that lies above 2400 cm^{-1} RPA and CIS produce two rather intense peaks, which contrasts with the experimental findings. The disagreement becomes more evident for the case of the broad, low intensity fifth band, which only TDDFT and TDA are able to restore.

For molecule **II**, azulene, experiment indicates that the absorption spectrum presents a quite complicated structure. From the theoretical point of view this molecule is quite interesting, since it belongs to the not so rare cases for which a HF description leads to a lowering of the point group symmetry.[83] In fact, due to the well-known overlocalization of electronic charge by HF theory, deviations from planarity are observed, resulting in a structure possessing C_s symmetry. This has already been discussed by Grimme.[84,85] DFT on the other hand is able to describe charge delocalization and predicts a planar C_{2v} structure. These differences in symmetry have a dramatic effect on the vibronic spectrum as can be readily seen in Figure 2. One notes that both RPA and CIS do not predict

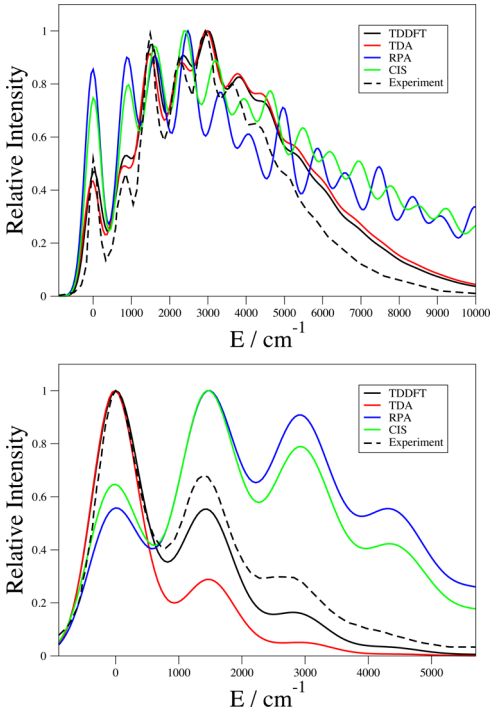

Figure 2. Comparison of the experimental and computed absorption spectrum of **II** (top) and **III** (bottom) using the 6-31+G(d) basis set.

the experimental shape of the spectrum, exhibiting a series of closely packed bands that have considerable intensity even at wavenumbers for which, experimentally, no structure is observed. As far as TDDFT and TDA are concerned, the agreement between theory and experiment is striking both in terms of band shapes and relative intensities. Both methods predict that the fifth peak is the most intense and can reproduce the fine, low intensity structure in the region above 3500 cm^{-1}. A comparison between TDDFT and TDA reveals that there is practically no difference between the two in terms of the positions of the band maxima nor the corresponding intensities; no deterioration of the overall shape of the spectrum takes place when neglecting deexcitations.

The exposition so far has been focused solely on hydrocarbons. Molecules **III** and **IV** represent chromophores that contain heteroatoms. Despite their structural differences, their absorption spectra are very similar in shape (see Figures 2 and 3). They are composed of three bands that progressively

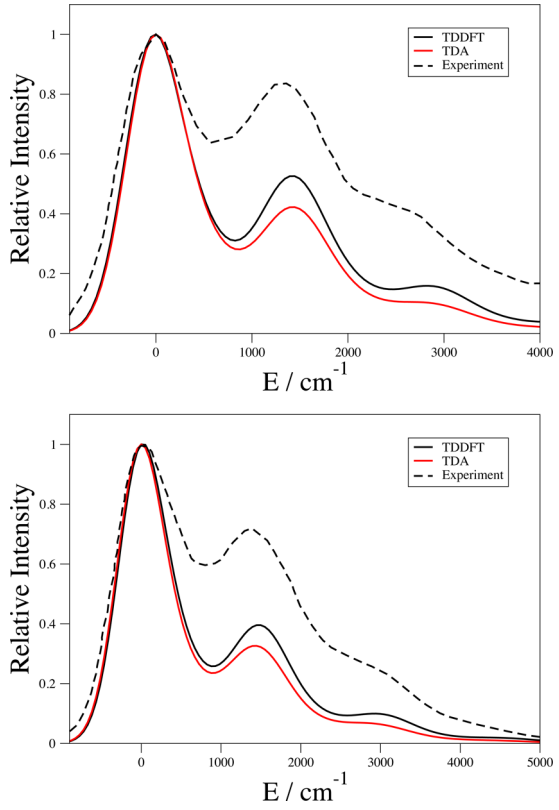

Figure 3. Comparison of the experimental and computed absorption (top) and emission (bottom) spectrum of **IV** using the 6-31+G(d) basis set.

decrease in intensity by passing to larger wavenumbers. For **III**, there exist important differences between TDDFT and RPA lines. RPA, in contrast to the experiment, predicts that the highest intensity band is the second one and, consequently, underestimates the first while TDDFT returns the correct ordering. Moreover, RPA shows a very well-defined, intense third band that is different compared to broad and of low intensity experimental one while the corresponding TDDFT band shape is again notably closer to what experiment predicts. More importantly, RPA shows an intense, artificial fourth band, which does not appear in the corresponding TDDFT spectrum. TDA clearly retains the shape of the TDDFT spectrum, lowering the intensities of the bands, the behavior of CIS is slightly more involved, leading to an increase in intensity of the first band; the contrary being observed for the other peaks. The fact that the TDA vibrational progression is less intense than its TDDFT counterpart is related to smaller variations of the geometry between the ground and excited states with TDA

dx.doi.org/10.1021/ct400597f | J. Chem. Theory Comput. 2013, 9, 4517−4525

than with TDDFT (see SI for numerical values). For molecule **IV**, the same trends with respect to the intensities and the band shapes can be seen for TDDFT and TDA, with both methods being able to capture the measured spectrum's shape for absorption as well as for emission.

As a last example, molecule **VI**, despite its simplicity offers a challenge to theory, especially when emission is concerned. The theoretical absorption and emission spectra are reported in Figure 4, along with the experimental ones. For absorption, the

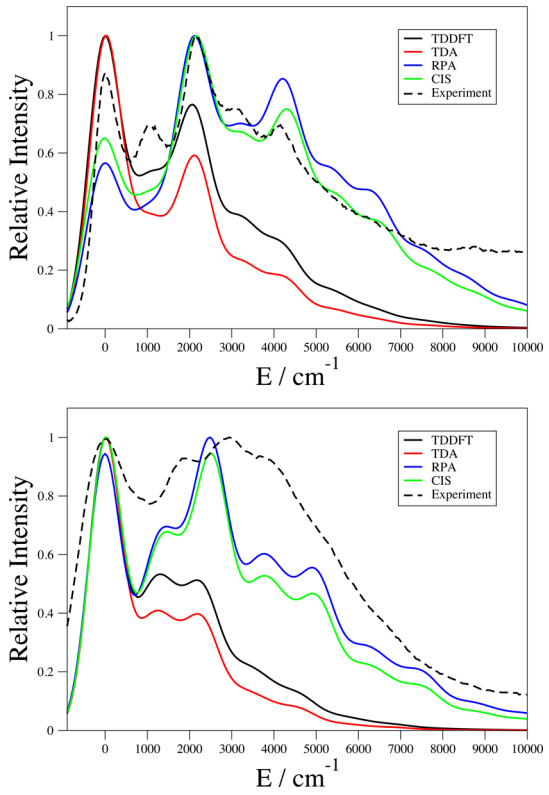

Figure 4. Comparison of the experimental and computed absorption (top) and emission (bottom) spectrum of **VI** using the 6-31+G(d) basis set.

experimental spectrum is composed of five bands. TDDFT and RPA are in disagreement in the positioning of the most intense band, the latter being in agreement with the experimental findings. Both methods fail to reproduce the separation between the two first bands. Interestingly, RPA is able to reproduce the shape of the last band while TDDFT shows a weak, shoulder-like band that does not fit to the experiment. Nonetheless, the RPA spectrum shows some artificial structure in the region above 5000 cm^{-1}, while TDDFT recovers the correct picture in that region. A comparison between TDDFT and TDA shows that the overall shape of the spectrum is unaltered, with only a slight shift of the band maxima, while the intensities are lowered by passing to the more approximate model. Turning our attention to the emission spectrum, it becomes clear that the disagreement between theory and experiment becomes even more pronounced than in the case of absorption. No method can be claimed to reproduce faithfully the shape of the experimental spectrum although the topology of the first band is accurately reproduced. Nevertheless, the positions of the three, not well resolved, bands that follow the first one cannot be reproduced by TDDFT nor RPA. Differences in intensity are clearly noticeable by comparing TDDFT and RPA, the latter leading to a great overestimation in the case of the third band maximum. The same problem that has been observed previously, namely the existence of artificial bands in the case of RPA for the high-energy part of the spectrum can also be found in the current case, in contrast to what TDDFT predicts. The TDA approximation does not alter the qualitative observations discussed for the case of TDDFT, leading only to a lowering of the intensities; a trend already noted above. For CIS, the shape of the emission spectrum is the same compared to the more accurate RPA one, while the intensities are underestimated for all bands except the first, for which the opposite behavior can be seen.

3.3. Functional Benchmarks. The relative performances of different functionals in reproducing experimental vibronic band shapes was of no immediate interest in this work. A benchmark study was nevertheless performed here in order to ensure that general conclusions can be drawn on the performance of TDA and to put forth emerging trends. In Figures 5 and 6, we show the results of benchmark calculations

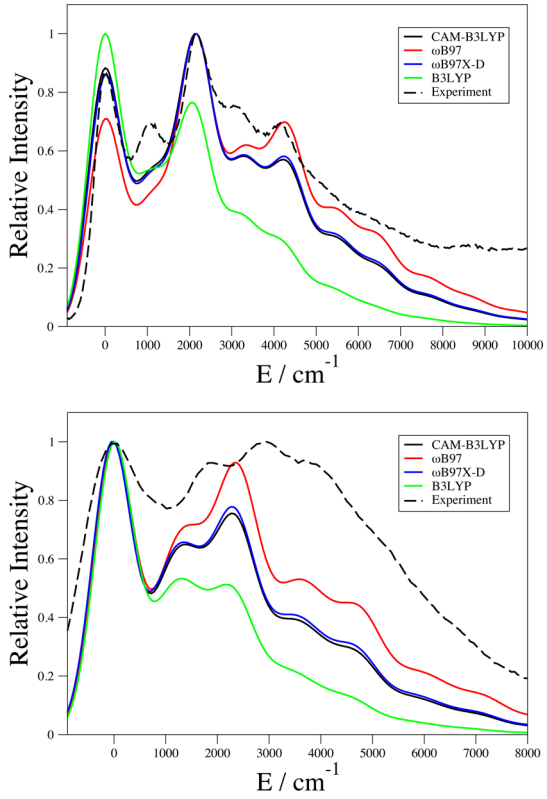

Figure 5. TDDFT/6-31+G(d) absorption (top) and emission (bottom) spectra of **VI** using several functionals.

performed for **VI** using three very popular long-range corrected functionals, CAM-B3LYP, ωB97, and ωB97X-D, combined with TDDFT and TDA. For both absorption and emission, variations in the relative intensities can be spotted, depending on the functional employed, but with small shifts for the position of the most well-defined, intense peaks. Most importantly, the band shape, for a given functional, does not change by passing from TDDFT to the more approximate TDA. This clearly suggests that the good performance of TDA in reproducing absorption and emission band shapes does not hold only for B3LYP but is independent of the chosen functional. Additionally, it can also be seen that the tendency of

dx.doi.org/10.1021/ct400597f | J. Chem. Theory Comput. 2013, 9, 4517−4525

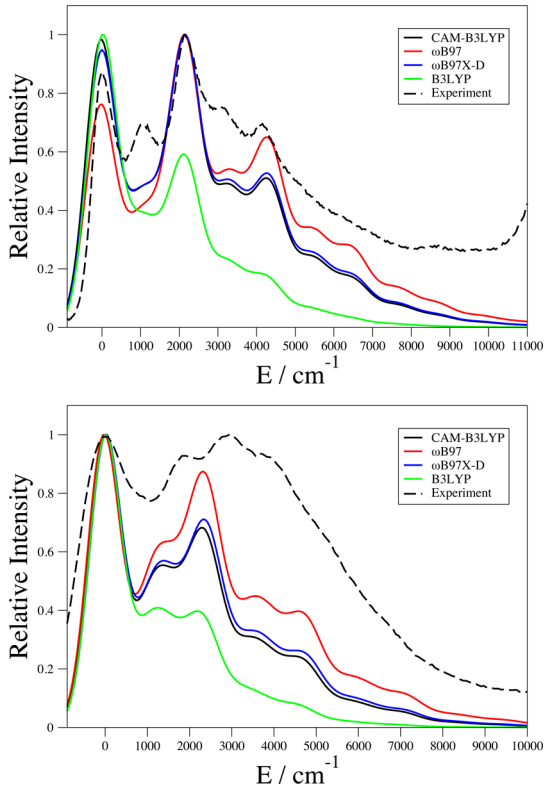

Figure 6. TDA/6-31+G(d) absorption (top) and emission (bottom) spectra of **VI** using several functionals.

TDA to underestimate the peak intensities is a quite general phenomenon. More extensive comparisons of experimental band shapes obtained with different functionals can be found in a previous work.[40]

4. CONCLUSIONS AND OUTLOOK

In this contribution, we have addressed for the first time the applicability of TDA in reproducing the experimental vibrationally resolved absorption and emission spectra along with the 0−0 energies of a series of medium-sized conjugated molecules. TDA is able to retain the good agreement between the experimental band shapes and the corresponding TDDFT ones, without any noticeable shifting of the positions of the peaks. Furthermore, it is evidenced that TDA leads to a lowering of the relative intensities in the vibronic progression compared to TDDFT for most cases considered. The only cases where TDA fails to reproduce the experimental shapes is when TDDFT fails to do so or when the peaks are of low intensity and not well resolved. For RPA and CIS methods the agreement is terms of spectral shapes and the positions of the absorption/emission maxima is satisfactory for the low energy part of the spectra, while for higher energies important discrepancies between both methods and experiment can be found, with a tendency to overestimate the experimental peak intensities in that region. With respect to the 0−0 energies, TDDFT gives errors ranging from 8% to 15% of the experimental values. TDA improves the agreement, reducing the error panel to 1−14%, but of course, this conclusion is limited to the B3LYP hybrid functional. For the case of RPA and CIS the error panel is much larger, resulting in a performance largely case dependent, with the omission of deexcitations leading to larger errors for the majority of the investigated cases.

The aforementioned findings clearly show that the neglect of deexcitations does not have the same effects on the quality of the obtained results with TDDFT and RPA methods. Moreover, RPA and CIS are probably inadequate for the simulation of vibrationally resolved electronic spectra as well as for the computation of 0−0 energies. On the other hand, TDA seems to be as reliable as TDDFT in reproducing vibrational signatures and seems to be a cost-effective candidate for the exploration of ES potential energy surfaces and properties or reactivity of large molecules,[86,87] directions which we intend to follow in the near future.

■ ASSOCIATED CONTENT

Supporting Information

Absorption and emission spectra for **V**, **VII**, and **VIII**. FC_{00} parameters and FC factors for all molecules. FC_{00} parameters and FC factors for the benchmarks. Data for the calculation of solvent shifts. TDDFT/TDA comparison with CAM-B3LYP, ωB97, and ωB97X-D for **VI**. This material is available free of charge via the Internet at http://pubs.acs.org.

■ AUTHOR INFORMATION

Corresponding Author

*E-mail: Denis.Jacquemin@univ-nantes.fr.

Notes

The authors declare no competing financial interest.

■ ACKNOWLEDGMENTS

The authors are indebted to the COST program CODECS and its members for support and many helpful discussions, respectively. A.C. thanks the European Research Council (ERC) for his postdoctoral grant (Marches project 278845). A.D.L. thanks the Q-Chem team for providing a development version of Q-Chem. D.J. acknowledges both the European Research Council (ERC) and the *Région des Pays de la Loire* for financial support in the framework of a Starting Grant (Marches 278845) and *recrutement sur poste stratégique*, respectively. This research used resources of (1) CCIPL (*Centre de Calcul Intensif des Pays de la Loire*) and (2) a local Troy cluster bought thanks to the financial support of the *Région des Pays de la Loire*.

■ REFERENCES

(1) Ullrich, C. *Time-Dependent Density-Functional Theory: Concepts and Applications*; Oxford University Press Inc.: New York, 2012; p 536.
(2) *Fundamentals of Time-Dependent Density Functional Theory*; Marques, M. A. L., Maitra, N. T., Nogueira, F. M. S., Gross, E. K. U., Eds.; Springer-Verlag: Berlin Heidelberg, 2012; p 591.
(3) *Time-Dependent Density Functional Theory*; Marques, M. A. L., Ullrich, C. A., Nogueira, F., Rubio, A., Eds.; Springer-Verlag: Berlin Heidelberg, 2006; p 625.
(4) Marques, M. A. L.; Gross, E. K. U. *Annu. Rev. Phys. Chem.* **2004**, *55*, 427−455.
(5) Grimme, S. Calculation of the Electronic Spectra of Large Molecules. In *Reviews in Computational Chemistry*; Lipkowitz, K. B., Larter, R., Cundari, T. R., Eds.; John Wiley & Sons, Inc.: Hoboken, NJ, 2004; Vol. *20*, pp 153−211.
(6) Onida, G.; Reining, L.; Rubio, A. *Rev. Mod. Phys.* **2002**, *74*, 601−659.
(7) Dreuw, A.; Head-Gordon, M. *Chem. Rev.* **2005**, *105*, 4009−4037.
(8) Barone, V.; Polimeno, A. *Chem. Soc. Rev.* **2007**, *36*, 1724−1731.

(9) Barone, V.; Improta, R.; Rega, N. *Acc. Chem. Res.* **2008**, *41*, 605−616.
(10) Neese, F. *Coord. Chem. Rev.* **2009**, *253*, 526−563.
(11) Jacquemin, D.; Perpète, E. A.; Ciofini, I.; Adamo, C. *Acc. Chem. Res.* **2009**, *42*, 326−334.
(12) Casida, M. E. *J. Mol. Struct. (THEOCHEM)* **2009**, *914*, 3−18.
(13) Baer, R.; Livshits, E.; Salzner, U. *Annu. Rev. Phys. Chem.* **2010**, *61*, 85−109.
(14) Casida, M. E.; Huix-Rottlant, M. *Annu. Rev. Phys. Chem.* **2012**, *63*, 287−323.
(15) Adamo, C.; Jacquemin, D. *Chem. Soc. Rev.* **2013**, *42*, 845.
(16) Casida, M. E. In *Time-Dependent Density-Functional Response Theory for Molecules*, Chong, D. P., Ed.; World Scientific: Singapore, 1995; Vol. *1*, pp 155−192.
(17) Nguyen, P. D.; Ding, F.; Ficher, S. A.; Liang, W.; Li, X. *J. Phys. Chem. Lett.* **2012**, *3*, 2898−2904.
(18) Li, X.; Smith, S. M.; Markevitch, A. N.; Romanov, D. A.; Levis, R. J.; Schlegel, H. B. *Phys. Chem. Chem. Phys.* **2005**, *7*, 233−239.
(19) Moss, C. L.; Isborn, C. M.; Li, X. *Phys. Rev. A* **2009**, *80*, 024503.
(20) Liang, W.; Isborn, C. M.; Lindsay, A.; Li, X.; Smith, S. M.; Levis, R. J. *J. Phys. Chem. A* **2010**, *114*, 6201−6206.
(21) Chapman, C. T.; Liang, W.; Li, X. *J. Phys. Chem. A* **2013**, *117*, 2687−2691.
(22) Runge, E.; Gross, E. K. U. *Phys. Rev. Lett.* **1984**, *52*, 997−1000.
(23) Dreuw, A.; Head-Gordon, M. *J. Am. Chem. Soc.* **2004**, *126*, 4007−4016.
(24) Maitra, N. T.; Zhang, F.; Cave, R. J.; Burke, K. *J. Chem. Phys.* **2004**, *120*, 5932−5937.
(25) Elliott, P.; Goldson, S.; Canuhai, C.; Maitra, N. T. *Chem. Phys.* **2011**, *391*, 110−119.
(26) Casida, M. E.; Casida, K. C.; Salahub, D. R. *Int. J. Quantum Chem.* **1998**, *70*, 933−941.
(27) Maitra, N. T. *J. Chem. Phys.* **2006**, *125*, 014110.
(28) Levine, B. G.; Ko, C.; Quenneville, J.; Martínez, T. J. *Mol. Phys.* **2006**, *104*, 1039−1051.
(29) Tapavicza, E.; Tavarnelli, I.; Rothlisberger, U.; Filippi, C.; Casida, M. E. *J. Chem. Phys.* **2008**, *129*, 124108.
(30) Bauernsschmitt, R.; Ahlrichs, R. *Chem. Phys. Lett.* **1996**, *256*, 454−464.
(31) Hirata, S.; Head-Gordon, M. *Chem. Phys. Lett.* **1999**, *314*, 291−299.
(32) Peach, M. J. G.; Williamson, M. J.; Tozer, D. J. *J. Chem. Theory Comput.* **2011**, *7*, 3578−3585.
(33) Peach, M. J. G.; Tozer, D. J. *J. Phys. Chem. A* **2012**, *116*, 9783−9789.
(34) Wang, Y.-L.; Wu, G.-S. *Int. J. Quantum Chem.* **2007**, *108*, 430−439.
(35) Richard, R. M.; Herbert, J. M. *J. Chem. Theory. Comput.* **2011**, *7*, 1296−1306.
(36) Hsu, C.-P.; Hirata, S.; Head-Gordon, M. *J. Phys. Chem. A* **2001**, *105*, 451−458.
(37) Cordova, F.; Doriol, L. J.; Ipatov, A.; Casida, M. E.; Filippi, C.; Vela, A. *J. Chem. Phys.* **2007**, *127*, 164111.
(38) Laurent, A. D.; Jacquemin, D. *Int. J. Quantum Chem.* **2013**, *113*, 2019−2039.
(39) Jacquemin, D.; Mennucci, B.; Adamo, C. *Phys. Chem. Chem. Phys.* **2011**, *13*, 16987−16998.
(40) Charaf-Eddin, A.; Planchat, A.; Mennucci, B.; Adamo, C.; Jacquemin, D. *J. Chem. Theory Comput.* **2013**, *9*, 2749−2760.
(41) Bousquet, D.; Fukuda, R.; Maitarad, P.; Jacquemin, D.; Ciofini, I.; Adamo, C.; Ehara, M. *J. Chem. Theory Comput.* **2013**, *9*, 2368−2379.
(42) Guido, C. A.; Knecht, S.; Kongsted, J.; Mennucci, B. *J. Chem. Theort Comput.* **2013**, *9*, 2209−2220.
(43) Dierksen, M.; Grimme, S. *J. Phys. Chem. A* **2004**, *108*, 10225−10237.
(44) Send, R.; Kühn, M.; Furche, F. *J. Chem. Theory Comput.* **2011**, *7*, 2376−2386.
(45) Jacquemin, D.; Planchat, A.; Adamo, C.; Mennucci, B. *J. Chem. Theory Comput.* **2012**, *8*, 2359−2372.
(46) Liu, J.; Liang, W. Z. *J. Chem. Phys.* **2011**, *135*, 184111.
(47) Liu, J.; Liang, W. Z. *J. Chem. Phys.* **2011**, *135*, 014113.
(48) Liu, J.; liang, W. Z. *J. Chem. Phys.* **2013**, *138*, 024101.
(49) Franck, J. *Trans. Faraday Soc.* **1926**, *21*, 536−542.
(50) Condon, E. *Phys. Rev.* **1928**, *32*, 858−872.
(51) Herzberg, G.; Teller, E. *Z. Phys. Chem. Abt. B* **1933**, *21*, 410−446.
(52) Santoro, F.; Improta, R.; Lami, A.; Bloino, J.; Barone, V. *J. Chem. Phys.* **2007**, *126*, 084509.
(53) Santoro, F.; Improta, R.; Lami, A.; Bloino, J.; Barone, V. *J. Chem. Phys.* **2007**, *126*, 184102.
(54) Santoro, F.; Lami, A.; Improta, R.; Bloino, J.; Barone, V. *J. Chem. Phys.* **2008**, *128*, 224311.
(55) Avila Ferrer, F. J.; Santoro, F. *Phys. Chem. Chem. Phys.* **2012**, *14*, 13549−13563.
(56) Biczysko, M.; Bloino, J.; Santoro, F.; Barone, V. In *Computational Strategies for Spectroscopy: From Small Molecules to Nano Systems*; Barone, V., Ed.; John Wiley & Sons, Inc.: Hoboken, NJ, 2012; Chapter 8, pp 361−443.
(57) Grimme, S.; Neese, F. *J. Chem. Phys.* **2007**, *127*, 154116.
(58) Hirata, S.; Lee, T. J.; Head-Gordon, M. *J. Chem. Phys.* **1999**, *111*, 8904−8912.
(59) Del Bene, J. E.; Ditchfield, R.; Pople, J. A. *J. Chem. Phys.* **1971**, *55*, 2236−2241.
(60) Foresman, J. B.; Head-Gordon, M.; Pople, J. A.; Frisch, M. J. *J. Phys. Chem.* **1992**, *96*, 135−149.
(61) Bouman, T. D.; Hansen, A. E. *Int. J. Quantum Chem. Symp.* **1989**, *23*, 381−396.
(62) Hansen, A. E.; Voight, B.; Rettrup, S. *Int. J. Quantum Chem.* **1983**, *23*, 595−611.
(63) Shao, Y.; Molnar, L. F.; Jung, Y.; Kussmann, J.; Ochsenfeld, C.; Brown, S.; Gilbert, A. T. B.; Slipchenko, L. V.; Levchenko, S. V.; O'Neil, D. P.; Distasio, R. A., Jr; Lochan, R. C.; Wang, T.; Beran, G. J. O.; Besley, N. A.; Herbert, J. M.; Lin, C. Y.; Van Voorhis, T.; Chien, S. H.; Sodt, A.; Steele, R. P.; Rassolov, V. A.; Maslen, P.; Korambath, P. P.; Adamson, R. D.; Austin, B.; Baker, J.; Bird, E. F. C.; Daschel, H.; Doerksen, R. J.; Dreuw, A.; Dunietz, B. D.; Dutoi, A. D.; Furlani, T. R.; Gwaltney, S. R.; Heyden, A.; Hirata, S.; Hsu, C.-P.; Kedziora, G. S.; Khalliulin, R. Z.; Klunziger, P.; Lee, A. M.; Liang, W. Z.; Lotan, I.; Nair, N.; Peters, B.; Proynov, E. I.; Pieniazek, P. A.; Rhee, Y. M.; Ritchie, J.; Rosta, E.; Sherrill, C. D.; Simmonett, A. C.; Subotnik, J. E.; Woodcock, H. L., III; Zhang, W.; Bell, A. T.; Chakraborty, A. K.; Chipman, D. M.; Keil, F. J.; Warshel, A.; Herhe, W. J.; Schaefer, H. F., III; Kong, J.; Krylov, A. I.; Gill, P. M. W.; Head-Gordon, M. *Phys. Chem. Chem. Phys.* **2006**, *8*, 3172−3191.
(64) Becke, A. D. *J. Chem. Phys.* **1993**, *98*, 5648−5652.
(65) Stephens, P. J.; Devlin, F. J.; Chabalowski, C. F.; Frisch, M. J. *J. Phys. Chem.* **1994**, *98*, 11623−11627.
(66) Chai, J.-D.; Head-Gordon, M. *J. Chem. Phys.* **2008**, *128*, 084106.
(67) Chai, J.-D; Head-Gordon, M. *Phys. Chem. Chem. Phys.* **2008**, *10*, 6615−6620.
(68) Yanai, T.; Tew, D.; Handy, N. *Chem. Phys. Lett.* **2004**, *393*, 51−57.
(69) Frisch, M. J.; Trucks, G. W.; Schlegel, H. B.; Scuseria, G. E.; Robb, M. A.; Cheeseman, J. R.; Scalmani, G.; Barone, V.; Mennucci, B.; Petersson, G. A.; Nakatsuji, H.; Caricato, M.; Li, X.; Hratchian, H. P.; Izmaylov, A. F.; Bloino, J.; Zheng, G.; Sonnenberg, J. L.; Hada, M.; Ehara, M.; Toyota, K.; Fukuda, R.; Hasegawa, J.; Ishida, M.; Nakajima, T.; Honda, Y.; Kitao, O.; Nakai, H.; Vreven, T.; Montgomery, Jr., J. A.; Peralta, J. E.; Ogliaro, F.; Bearpark, M.; Heyd, J. J.; Brothers, E.; Kudin, K. N.; Staroverov, V. N.; Kobayashi, R.; Normand, J.; Raghavachari, K.; Rendell, A.; Burant, J. C.; Iyengar, S. S.; Tomasi, J.; Cossi, M.; Rega, N.; Millam, J. M.; Klene, M.; Knox, J. E.; Cross, J. B.; Bakken, V.; Adamo, C.; Jaramillo, J.; Gomperts, R.; Stratmann, R. E.; Yazyev, O.; Austin, A. J.; Cammi, R.; Pomelli, C.; Ochterski, J. W.; Martin, R. L.; Morokuma, K.; Zakrzewski, V. G.; Voth, G. A.; Salvador, P.; Dannenberg, J. J.; Dapprich, S.; Daniels, A. D.; Farkas, Ö.; Foresman, J. B.; Ortiz, J. V.; Cioslowski, J.; Fox, D. J. *Gaussian 09*, Revision C.01; Gaussian, Inc.: Wallingford, CT, 2009.

(70) Baker, J. *J. Comput. Chem.* **1986**, *7*, 385−395.
(71) Santoro, F. *FCclasses, a Fortran 77 code.* Available at http://village.pi.iccom.cnr.it/en/Software (accessed Aug. 16, 2013).
(72) Valeur, B. *Molecular Fluorescence: Principles and Applications*; Wiley-VCH: Weinheim, 2002.
(73) Avila Ferrer, F. J.; Cerezo, J.; Stendardo, E.; Improta, R.; Santoro, F. *J. Chem. Theory Comput.* **2013**, *9*, 2072−2082.
(74) Tomasi, J.; Mennucci, B.; Cammi, R. *Chem. Rev.* **2005**, *105*, 2999−3093.
(75) Improta, R.; Barone, V.; Sclamani, G.; Frisch, M. J. *J. Chem. Phys.* **2006**, *125*, 054103.
(76) Ferguson, J.; Reeves, L. W.; Schneider, W. G. *Can. J. Chem.* **1957**, *35*, 1117−1123.
(77) Lambert, Wm. R.; Felker, P. M.; Zewail, A. H. *J. Chem. Phys.* **1981**, *75*, 5958−5960.
(78) Lou, Y.; Chang, J.; Jorgensen, J.; Lemal, D. M. *J. Am. Chem. Soc.* **2002**, *124*, 15302−15307.
(79) Scholz, R.; Kobitski, A. Y.; Kampen, T. U.; Schreiber, M.; Zahn, D. R. T.; Jungnickel, G.; Elstner, M.; Sternberg, M.; Fraunheim, T. *Phys. Rev. B* **2000**, *61*, 13659−13669.
(80) Berlman, I. B. *Handbook of Fluorescence Spectra of Aromatic Molecules*, 2nd ed.; Academic Press: New York, 1971; pp 258.
(81) Du, H.; Fuh, R. A.; Li, J.; Corkan, A.; Lindsey, J. S. *Photochem. Photobiol.* **1998**, *68*, 141−142. Spectra available at http://omlc.ogi.edu/spectra/PhotochemCAD/ (accessed Aug. 16, 2013) and at http://www.fluorophores.tugraz.at/ (accessed Aug. 16, 2013).
(82) Mühlpfordt, A.; Schanz, R.; Ernsting, N. P.; Farztdinov, V.; Grimme, S. *Phys. Chem. Chem. Phys.* **1999**, *1*, 3209−3218.
(83) Jacquemin, D.; Perpète, E.A .; Assfeld, X.; Scalmani, G.; Frisch, M. J.; Adamo, C. *Chem. Phys. Lett.* **2007**, *438*, 208−212.
(84) Grimme, S. *Chem. Phys. Lett.* **1993**, *201*, 67−74.
(85) Dierksen, M.; Grimme, S. *J. Chem. Phys.* **2004**, *120*, 3544−3554.
(86) Monari, A.; Rivail, J. L.; Assfeld, X. *Acc. Chem. Res.* **2013**, *46*, 596−603.
(87) Jurinovich, S.; Degano, I.; Mennucci, B.. *J. Phys. Chem. B* **2012**, *116*, 13344−13352.